BJR
© 2023 The Authors. Published by the British Institute of Radiology
https://doi.org/10.1259/bjr.20220686

Received: 13 July 2022 | Revised: 05 October 2022 | Accepted: 07 November 2022 | Published online: 08 December 2022

Cite this article as:
Diab R, Chang D, Zhu C, Levitt MR, Aksakal M, Zhao H-L, et al. Advanced cross-sectional imaging of cerebral aneurysms. *Br J Radiol* (2023) 10.1259/bjr.20220686.

REVIEW ARTICLE

Advanced cross-sectional imaging of cerebral aneurysms

[1]RAWAN DIAB, BS, [2]DANDAN CHANG, MD, [2]CHENGCHENG ZHU, PhD, [2,3,4,5]MICHAEL R. LEVITT, MD, [2]MEHMET AKSAKAL, MD, [6]HUI-LIN ZHAO, MD, PhD, [7]THIEN J. HUYNH, MD MSc, [8]GRISELDA ROMERO-SANCHEZ, MD and [2,9]MAHMUD MOSSA-BASHA, MD

[1]American University of Beirut School of Medicine, Beirut, Lebanon
[2]Department of Radiology, University of Washington, Seattle, United States
[3]Department of Neurosurgery, University of Washington, Seattle, United States
[4]Department of Mechanical Engineering, University of Washington, Seattle, United States
[5]Stroke and Applied Neurosciences, University of Washington, Seattle, United States
[6]Deparment of Radiology, Renji Hospital, Shanghai, China
[7]Department of Radiology, Mayo Clinic-Jacksonville, Jacksonville, United States
[8]Department of Radiology, Instituto Nacional de Ciencias Medicas y Nutricion Salvador Zubiran, Mexico City, Mexico
[9]Department of Radiology, University of North Carolina-Chapel Hill, Chapel Hill, United States

Address correspondence to: Dr Mahmud Mossa-Basha
E-mail: *mmossab@uw.edu*

ABSTRACT

While the rupture rate of cerebral aneurysms is only 1% per year, ruptured aneurysms are associated with significant morbidity and mortality, while aneurysm treatments have their own associated risk of morbidity and mortality. Conventional markers for aneurysm rupture include patient-specific and aneurysm-specific characteristics, with the development of scoring systems to better assess rupture risk. These scores, however, rely heavily on aneurysm size, and their accuracy in assessing risk in smaller aneurysms is limited. While the individual risk of rupture of small aneurysms is low, due to their sheer number, the largest proportion of ruptured aneurysms are small aneurysms. Conventional imaging techniques are valuable in characterizing aneurysm morphology; however, advanced imaging techniques assessing the presence of inflammatory changes within the aneurysm wall, hemodynamic characteristics of blood flow within aneurysm sacs, and imaging visualization of irregular aneurysm wall motion have been used to further determine aneurysm instability that otherwise cannot be characterized by conventional imaging techniques. The current manuscript reviews conventional imaging techniques and their value and limitations in cerebral aneurysm characterization, and evaluates the applications, value and limitations of advanced aneurysm imaging and post-processing techniques including intracranial vessel wall MRA, 4D-flow, 4D-CTA, and computational fluid dynamic simulations.

INTRODUCTION

Unruptured intracranial aneurysms (UIAs) are prevalent in 3–5% of the population.[1] Although the overall risk of rupture is low at 1% annually, aneurysmal rupture varies by individual and carries high morbidity and mortality. Around 27% of patients who develop subarachnoid hemorrhage (SAH) may die within one year.[2] The treatment of intracranial aneurysms whether by surgical clipping or endovascular treatment carries potential risks of morbidity and mortality of around 2–5%.[3] Considering that a majority of UIAs remain asymptomatic, and in order to maximize risk-to-benefit, it is essential to identify UIAs at high risk of rupture. Several factors have been included in risk stratification scores including patient-specific and aneurysm-specific characteristics. Such scores include the PHASES score which provides a five-year rupture risk of an aneurysm based on the following parameters: ethnicity, hypertension, age, aneurysm diameter, prior SAH from another ruptured aneurysm and site of aneurysm origin.[4] This scoring system, however, may not be routinely used clinically and relies heavily on aneurysm size, limiting its value in small-sized aneurysms. Furthermore, many ruptured aneurysms may be small and have a low PHASES score.[5–7] PHASES also does not take into account certain patient factors such as smoking, which have been linked to UIA rupture.[8]

Imaging is a cornerstone in the evaluation of intracranial aneurysms. Conventional luminal imaging techniques include computed tomography angiography (CTA),

magnetic resonance angiography (MRA), and catheter angiography.[9] For intracranial vascular diseases, including aneurysms, visualization of the vessel wall is of great importance, considering it is the primary site of pathologic involvement. Advanced imaging techniques that assess flow dynamics and associated wall shear characteristics also can provide valuable pathophysiological data that is not otherwise available with conventional cross-sectional imaging approaches. Hence, new imaging and post-processing techniques have been developed, including high-resolution vessel wall MRI (HR-VWI) and 4D-flow MRI, and computational fluid dynamics (CFD) simulations. These imaging modalities will be discussed in this review to highlight their potential utility in the evaluation of intracranial aneurysms.

Conventional CT and MR luminal imaging techniques

The conventional imaging modalities used for the evaluation of intracranial aneurysms include CTA, MRA, and catheter angiography.[10] Although catheter angiography is considered the gold standard for vasculopathy diagnosis and characterization, it is not often used as a first line approach since it is invasive, expensive and has limited availability compared to MRA and CTA.[11] It is also associated with rare procedural risks including stroke, vascular access complications, and contrast-induced nephropathy.[12]

MRA and CTA are usually the first-line imaging techniques for screening of intracranial aneurysms. For aneurysms greater than 3 mm in maximum diameter, CTA has a sensitivity between 77 and 97% and specificity between 87.5 and 100%, whereas MRA has a sensitivity of 70–99% and a specificity of 100%. For aneurysms smaller than 3 mm, both sensitivities of CTA and MRA drop to as low as 40%.[13,14] One study reviewing 401 aneurysm patients with SAH who underwent both CTA and DSA found that CTA sensitivity for aneurysms < 5 mm was 57.6%, and dropped to 45% for aneurysms originating on the internal carotid artery.[15] In patients with acute or severe chronic renal insufficiency, CTA may be relatively contraindicated due to the risk of contrast-induced acute kidney injury; however, this is an area of continued evolution of understanding.[16,17] Non-contrast TOF-MRA can be used instead in these subsets of patients. However, the advantage of CTA over MRA is that it takes less time to perform is easier to use on critically ill patients, and is more widely available.[18]

Vessel wall MRI

HR-VWI is a reliable advanced imaging modality that complements traditional imaging in the evaluation of intracranial aneurysms.[19,20] Not only can HR-VWI evaluate the lumen as or more accurately than conventional luminal imaging methods,[21] it allows for direct imaging of vessel wall abnormalities that might not otherwise be detected with conventional techniques.[22–24] HR-VWI can improve intracranial vasculopathy differentiation compared to conventional methods.[25–27] In a recent survey of the American Society of Neuroradiology membership, 52% of respondents indicated performance of HR-VWI in their clinical practices, 72% utilizing the technique at least 1–2 times per month, and almost 40% applying the technique to aneurysm characterization for instability.[28]

HR-VWI can accurately assess aneurysm size and morphology compared to 3D-DSA as a reference standard and it outperformed 3D-Time of Flight (TOF) MRA (coefficient of variance was 6.26% for HR-VWI *vs* 15.54% for TOF-MRA).[29] In addition, HR-VWI can visualize potential intraluminal thrombus, which may have critical treatment and pathophysiological implications.[29]

Although several different HR-VWI protocols have been described,[30–33] the main principle is the suppression of intraluminal blood and extraluminal CSF, such that the focus of the image is the vessel wall itself using sufficiently small-sized voxels to accurately visualize and assess the normal vessel wall of medium-sized arteries. Both sufficient signal-to-noise and spatial resolution are necessary for appropriate evaluation, considering the tortuosity of the small intracranial arteries and their thin walls.[19] While HR-VWI can be performed at lower field strengths, its optimal performance is using at least 3.0-Tesla MRI field strength systems.[34] A comparison of performance of 3-Tesla and 7-Tesla HR-VWI of 29 patients with 29 unruptured intracranial aneurysms showed that 7 T scans had significantly better aneurysm wall visualization relative to 3 T ($p = 0.003$).[35] Aneurysm wall thickness (AWT) was 15% thinner on 7 T compared to 3 T ($p < 0.001$), and wall sharpness was 57% higher on 7 T ($p < 0.001$).[35] 7T-MRI HR-VWI improvements were due to improved signal-to-noise ratio and spatial resolution (0.4 mm isotropic resolution at 7 T vs ~0.6 mm isotropic resolution at 3 T).[35–37] 7 T MRI systems, however, are limited to only a few centers.

Studies of surgically excised aneurysm samples showed that 2D HR-VWI vessel wall measurements were inaccurate when compared to light microscopy histological measurements, with overestimation of aneurysmal wall thickness (AWT) as wall thickness decreased. Measurements were significantly different for AWT at the dome (0.24 ± 0.06 mm *vs* 0.30 ± 0.068 mm for HR-VWI, $p = 0.0078$) and neck (0.25 ± 0.07 mm *vs* 0.29 ± 0.07 mm for HR-VWI, $p = 0.0469$) of the aneurysm.[38] However, this study concluded that inaccuracies were minimal and that AWT can be measured using HR-VWI provided that the measurement ranges are defined by maximum MR resolution ranging from 0 to 1.2 mm are used.

Despite this limitation, vessel wall thickness can be assessed qualitatively by experienced neuroradiologists and was shown to correlate with UIA instability. Hartman et al[39] evaluated the association between the PHASES score and aneurysmal wall enhancement (AWE) and wall thinning on HR-VWI. The study showed the degree of wall thinning was significantly greater in the higher risk group (PHASES>3) (9.2% vs 0%, $p = 0.044$).[39]

Aneurysm wall enhancement (AWE) is one of the most studied aneurysm characteristics and has shown associations with aneurysm rupture and aneurysm instability[35,39–46] (Figure 1). AWE is an indication of an underlying inflammatory process as shown through histopathological studies. In several studies,

Figure 1. 62-year-old male who presented with frequent headaches. 3D rotational angiogram of the right ICA (A) shows a right MCA trifurcation unruptured saccular aneurysm (arrow). Sagittal T_1-weighted pre- (B) and post-contrast (C) High-resolution vessel wall MRI (HR-VWI) demonstrates aneurysm wall enhancement (AWE) (arrowhead), which is shown to be an important indicator of rupture/vulnerability. The aneurysm was treated with endovascular coil embolization.

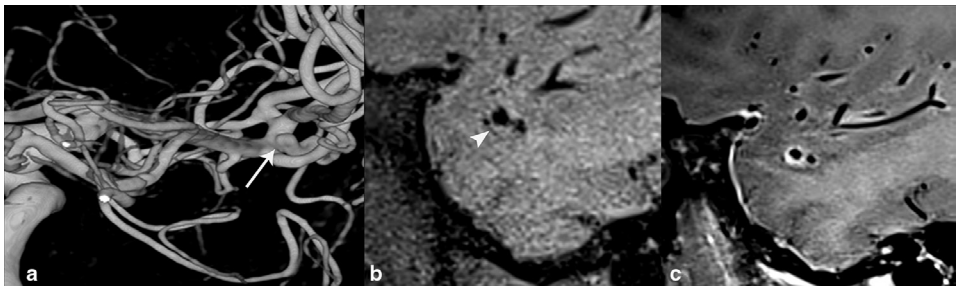

histological analysis was performed of aneurysms that showed AWE on HR-VWI. These studies revealed increased myeloperoxidase activity, neovascularization, presence of vasa vasorum, and macrophage infiltration.[47,48] Another study showed that UIA walls were deficient in elastin.[49] In addition, UIAs with focal enhancement showed thinner walls compared to those with circumferential enhancement whereby the histopathological analysis revealed thick walls, decreased elastic fibers, and decreased cellularity.[50] However, aneurysms with focal enhancement were more associated with atherosclerosis than those with circumferential enhancement.[51]

Artifactual enhancement, or "pseudoenhancement" on 3D post-contrast T_1-weighted HR-VWI can result from non-suppression of blood signal in the setting of slow or in-plane flow, especially in aneurysm sacs, and can mimic pathological enhancement[31,33] (Figure 2). A recent study compared AWE on conventional 3D-TSE and motion-sensitive-driven-equilibrium (MSDE) blood-suppressed 3D-TSE T1 post-contrast sequences, each performed on the same UIA patients, and found AWE on 10/30 conventional and 2/30 MSDE acquisitions ($p < .0001$).[31] Similarly, a recent study evaluated image quality comparing DANTE blood and CSF-suppressed 3D-TSE and conventional 3D-TSE post-contrast T_1-weighted acquisitions performed on the same patients, and found significant image quality improvement, reduced artefact and improved blood suppression and lesion assessment when DANTE suppression was incorporated.[33]

To measure AWE, qualitative and quantitative approaches have been developed. Qualitatively, some studies have graded AWE as strong/avid, mild, or none, compared to intracranial enhancing structures, such as the pituitary infundibulum[34]; strong enhancement is enhancement at or above the degree of enhancement of the infundibulum, mild enhancement is to a degree less than the infundibulum, and none is enhancement that does exceed the degree of enhancement of the normal arterial wall. Other studies have divided AWE into three categories: focal enhancement, thin circumferential, and thick circumferential.[40] Focal enhancement was defined as enhancement involving a specific portion of the aneurysm like the neck or dome. Circumferential enhancement is enhancement involving the entire aneurysm and is further subdivided into thin (<1 mm) and thick (>1 mm). In a study on UIA ($n = 307$),[40] thick circumferential enhancement exhibited the highest specificity (84.4%; 233/276; 95% CI: 80.1–88.7%; $p = .02$) and negative-predictive value (94.3%; 233/247) for differentiating stable and unstable lesions. Moreover, the results demonstrated a significant association between thick circumferential enhancement and aneurysm instability ($p = .0001$). Hartman et al[39] showed that aneurysms with greater risk of rupture (PHASES>3, $n = 38$) were more likely to show enhancement compared to aneurysms of lower rupture risk (PHASES≤3, $n = 27$) (42.1% vs 14.8%, $p = 0.022$).

As for quantitative methods, two approaches have been described.[9,41] The wall enhancement index (WEI) quantitates

Figure 2. 45-year-old male undergoing evaluation of aneurysm. Sagittal T_1-weighted pre-contrast HR-VWI (A) shows right MCA bifurcation aneurysm (short arrow). Sagittal conventional T1-SPACE post-contrast (B) shows multifocal AWE (arrowheads), which is not seen on T1-DANTE-SPACE blood-suppressed acquisition (C). The wall signal seen in (B) represents flow artefact mimicking AWE.

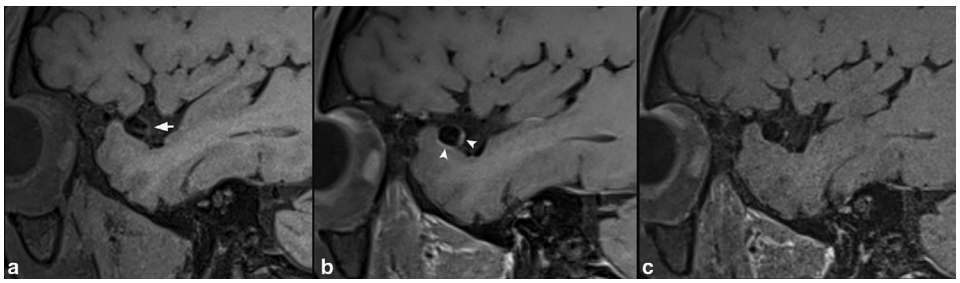

wall enhancement by comparing pre- and post-contrast signal intensity, while the aneurysm enhancement integral (AEI) compares this ratio to white matter enhancement.[41]

The second method compares aneurysm wall to pituitary infundibulum enhancement.[9] In a recent prospective cohort study with 273 UIA in 225 patients, both AWE pattern and WEI were shown to be independently associated with symptomatic (sentinel headache or oculomotor nerve palsy) UIAs.[41] The combination of the two had a sensitivity and specificity of 95.7% and 73.4%, respectively, for identifying symptomatic aneurysms. Several other studies have also identified AWE as an independent marker for aneurysm instability.[42,44,45]

Surrogates for rupture such as aneurysm growth, aneurysm diameter, and mass effect are associated with AWE on HR-VWI. In a study of 108 aneurysms, 87% (27/31) of the unstable aneurysms showed circumferential AWE as compared to 28.6% (22/77) of stable aneurysms ($p < 0.0001$).[52] Unstable aneurysms were those that showed growth, were symptomatic, or had ruptured. In the evaluation of 61 aneurysms with HR-VWI, Liu et al[44] found aneurysm size to be independently associated with AWE (OR 2.46 per mm increase). For aneurysms measuring <7 mm, however, 12% exhibited AWE. A recent meta-analysis which included 505 aneurysms confirmed that AWE was associated with aneurysm instability (OR 20; 95% CI 6.4–62.1).[53] While AWE is significantly more frequent in symptomatic, unstable, ruptured or growing aneurysms as compared to stable UIAs, it may also be seen in stable UIAs. The above meta-analysis found that the lack of AWE was a strong predictor for aneurysm stability.[53] More than 90% of saccular aneurysms without circumferential wall enhancement remain unruptured and asymptomatic.[52]

AWE of fusiform aneurysms differs from that seen with saccular aneurysms.[37] In one small study, all fusiform aneurysms (11/11) showed AWE, almost all of which was diffuse enhancement (Figure 3), compared to 57% (12/21) of saccular aneurysms showing enhancement, 75% of which was localized, focal enhancement. The increased enhancement frequency and extent in fusiform aneurysms correlates with increased aneurysm growth rate (6% *vs* 3% per year, respectively) and increased rupture rate (3% vs.<1% per year, respectively), compared to saccular aneurysms.[54,55]

Another utility of HR-VWI is its ability to identify the culprit aneurysm in the setting of acute SAH and aneurysm multiplicity (Figure 4). SAH is most often caused by a ruptured aneurysm, but in 30% of SAH cases, multiple aneurysms are present.[56] The identification of the culprit aneurysm is needed to guide treatment. When several aneurysms are present, AWE can identify the most likely involved aneurysm.[45,57] This is of added value since the location of SAH does not always identify the responsible aneurysm. Studies have shown that ruptured aneurysms are associated with increased wall enhancement and increased inflammatory cells on histopathological analysis.[58] However, a recent study[59] including patients with SAH suggests that the role of HR-VWI in the identification of the culprit aneurysm is subject to limitations. In this study, aneurysm rupture was estimated based on distribution of SAH and aneurysmal wall characteristics on HR-VWI. Confirmation of the aneurysm rupture site was performed intraoperatively during the surgical clipping. Interestingly, the accuracy rate of rupture site identification was 69.2%. The remaining percentage of cases demonstrated enhancement of the unruptured aneurysm to a greater degree than the actual ruptured aneurysm. One possible cause for this is the presence of atherosclerosis in the vessel containing the unruptured aneurysm. Thus, HR-VWI may be used in combination with other factors for the identification of the culprit aneurysm, but must be interpreted with caution as a standalone biomarker.

AWE on HR-VWI can serve as a marker for treatment response for UIAs. A recent randomized controlled trial longitudinally imaging UIAs with AWE at baseline, found that in those aneurysms treated with atorvastatin, there was significantly reduced quantitative AWE between baseline and 6-month follow-up ($p < .01$), while there was no significant reduction of AWE in the placebo group ($p = .27$).[43] AWE was significantly lower in the atorvastatin group, compared to placebo ($p = .02$). The changes in serum inflammatory markers (IL-6, c-reactive protein, and tumor-necrosis-factor-α) mirrored the changes in AWE, with significant reductions in levels after 6 month atorvastatin treatment (p = .033,.049, and.023, respectively). There were no changes in aneurysm morphology or size, supporting AWE on HR-VWI as a potential better marker for treatment response than aneurysm morphology.

Figure 3. 66-year-old male who had an incidentally found aneurysm. CTA head sagittal multiplanar reformat (A),shows a short segment fusiform basilar artery aneurysm (short arrow). Sagittal T_1-weighted pre- (B) and post-contrast (C) HR-VWI demonstrate AWE of the aneurysm (arrowheads). The aneurysm was subsequently treated with endovascular stenting.

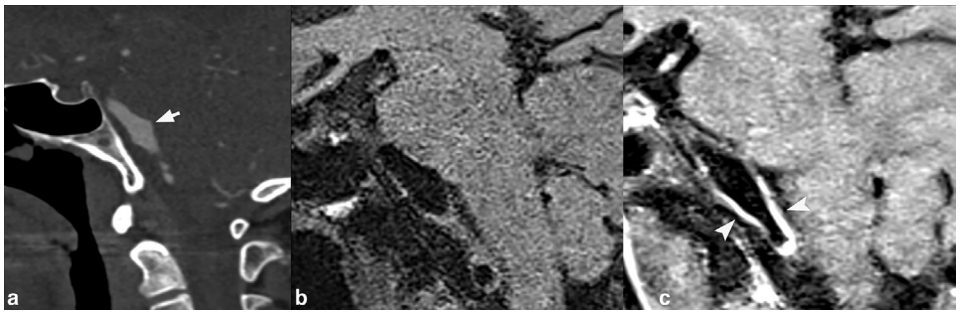

Figure 4. 42-year-old patient who presented with severe headache. On axial non-contrast CT head (A), there is subarachnoid hemorrhage in the left suprasellar cistern. On CTA head coronal reconstruction (B), cone-shaped outpouching projecting from the superior aspect of the left carotid terminus (arrow) was presumed to represent infundibulum due to its configuration and the appearance of a branch artery arising from its apex. Coronal T_1-weighted pre- (C) and post-contrast (D) HR-VWI redemonstrates the cone-shaped outpouching that shows AWE at its dome, a finding associated with aneurysm vulnerability, and not present in infundibula. 3D digital subtraction angiographic reconstruction (E) confirms the superiorly projecting carotid terminus outpouching does not have branches and represents aneurysm. The ruptured aneurysm was subsequently treated surgically.

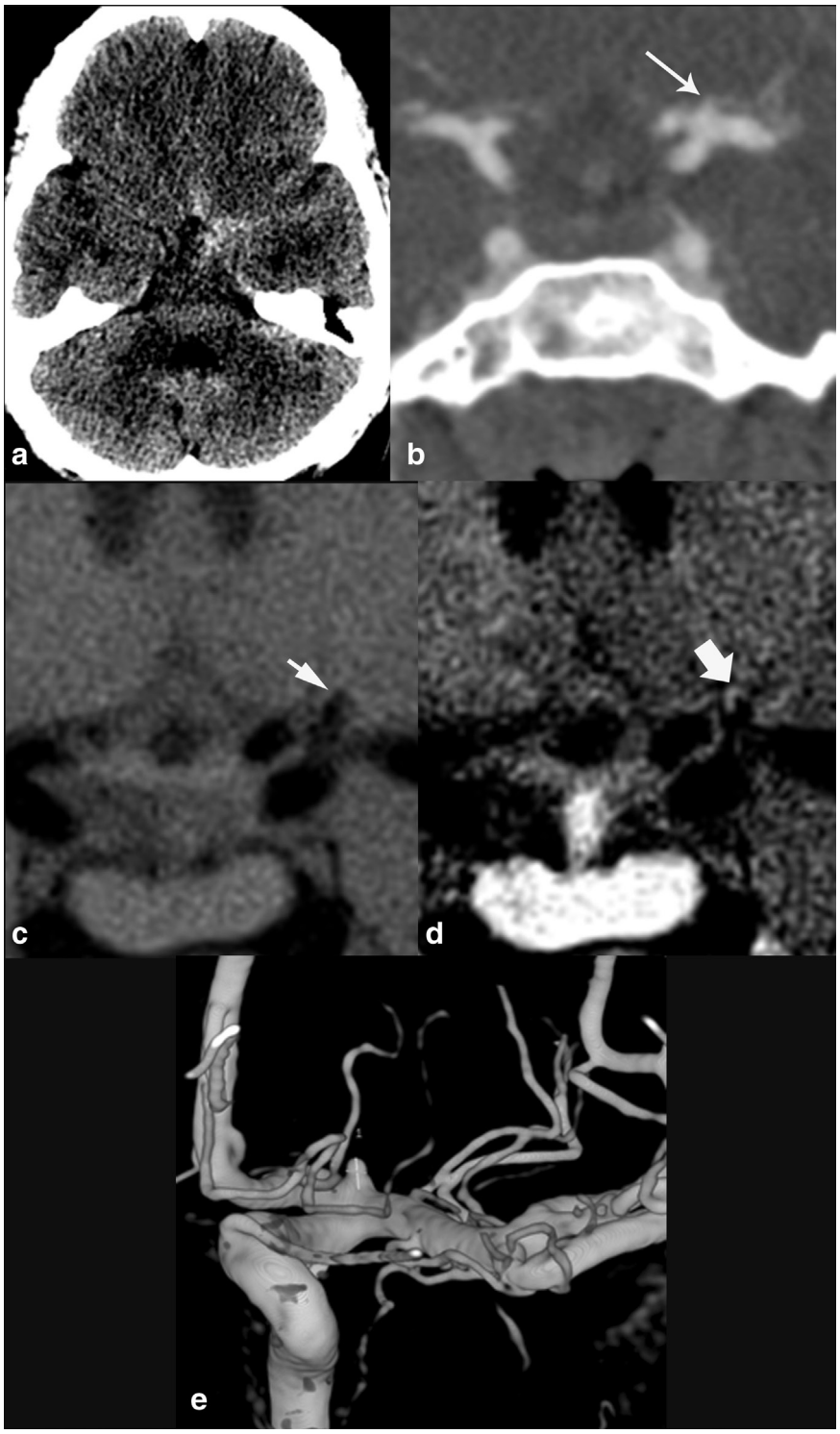

Figure 5. 25 year old female who presented with severe headache and altered mental status. On axial non-contrast CT head (A), there was diffuse basilar subarachnoid hemorrhage and intraventricular blood in the left temporal horn. 3D rotational angiogram of the left vertebral artery (B), demonstrated posteriorly directed, lobulated left superior cerebellar artery aneurysm (short arrow). After the ruptured aneurysm was treated with coil embolization, sagittal T_1-weighted pre- (C) and post-contrast (D) HR-VWI demonstrated right M1 MCA segment wall enhancement. This finding is significantly associated with subsequent angiographic vasospasm. CTA coronal MIP (E) obtained two days after HR-VWI performance, when compared to initial presentation CTA coronal MIP (F), showed diffuse angiographic vasospasm.

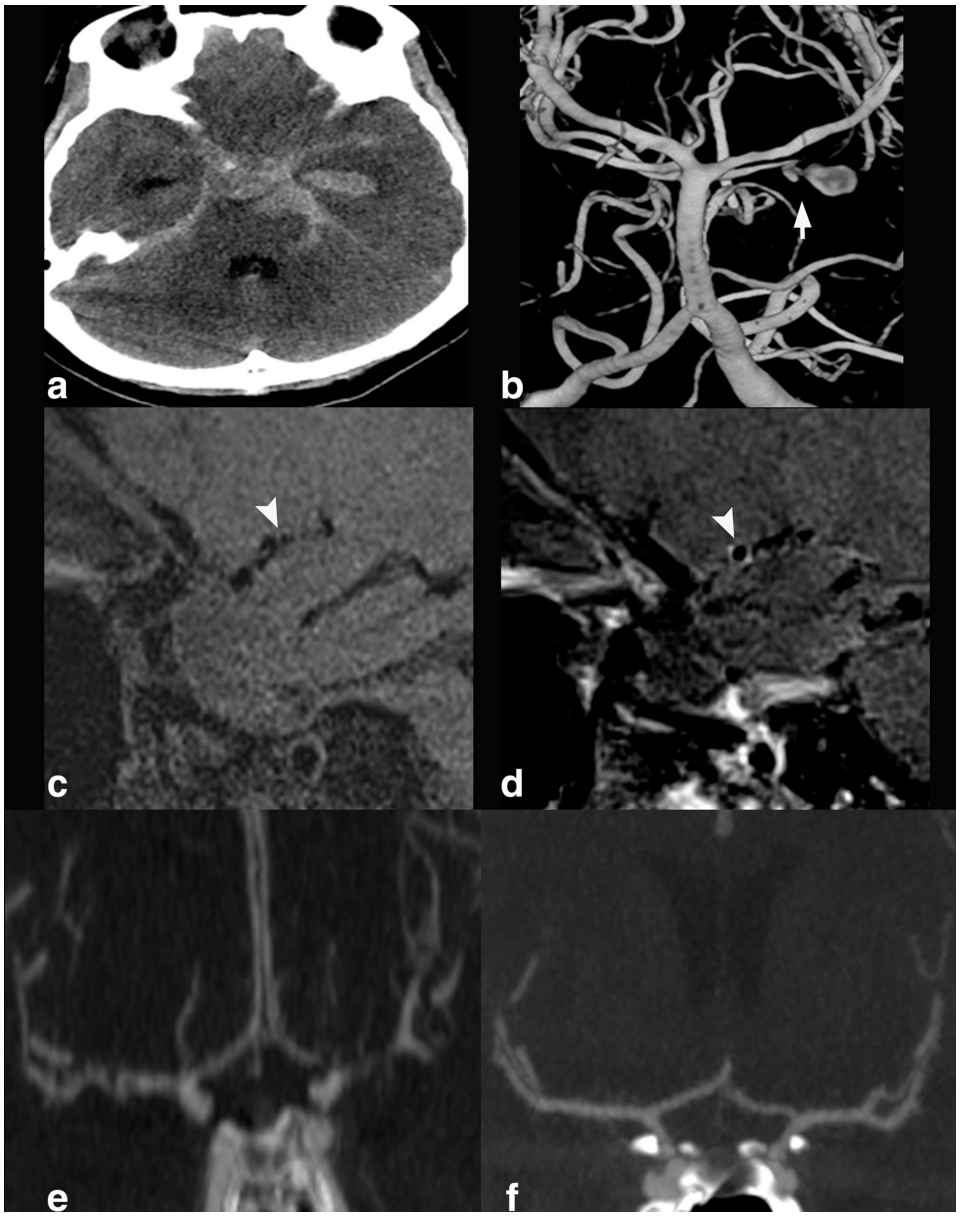

AWE has also been used as a potential imaging marker for angiographic vasospasm after aneurysmal SAH (Figure 5). One study prospectively evaluated 29 patients with 30 treated aneurysms (22 ruptured and eight unruptured) with HR-VWI immediately after intervention.[60] Ruptured aneurysm cases had a significantly higher number of enhancing arterial segments than unruptured cases (29.9% vs 7.2%, odds ratio 5.5, 95% CI 2.2–13.7), likely due to the inflammatory nature of SAH. For ruptured aneurysms, the presence of AWE was significantly associated with the development of angiographic vasospasm, when controlling for modified Fischer scale score of SAH (adjusted odds ratio 3.9, 95% CI 1.7–9.4). Another study evaluated the correlation of wall enhancement and delayed cerebral ischemia in 32 patients with aneurysmal SAH stratified into high- and low-risk based on Vasograde score, evaluated at two time points with HR-VWI, and found wall enhancement was significantly more common in the high-risk group at the early HR-VWI acquisition (36.7% vs 20%, $p = 0.024$).[61] Wall enhancement on both the early and late HR-VWI were associated with delayed cerebral ischemia development. Future comparison between HR-VWI and

Figure 6. 48 year old with partially thrombosed right MCA aneurysm. Coronal MIP CTA reconstruction (A) shows patent aneurysm lumen projecting inferiorly from the MCA trifurcation (short arrow), with subtle boundary representing the margin of the thrombosed aneurysm sac (arrowheads). On axial T_2-weighted HR-VWI (B), aneurysm sac thrombus shows heterogeneous signal with central T2 hypointensity and peripheral hyperintensity. On sagittal T_1-weighted HR-VWI (C), patent aneurysm lumen projecting inferiorly from the MCA (short arrow), with inferior aneurysm heterogeneous intraluminal thrombus (arrowheads) are appreciated. On sagittal post-contrast T_1-weighted HR-VWI (D), there is AWE (thick arrows).

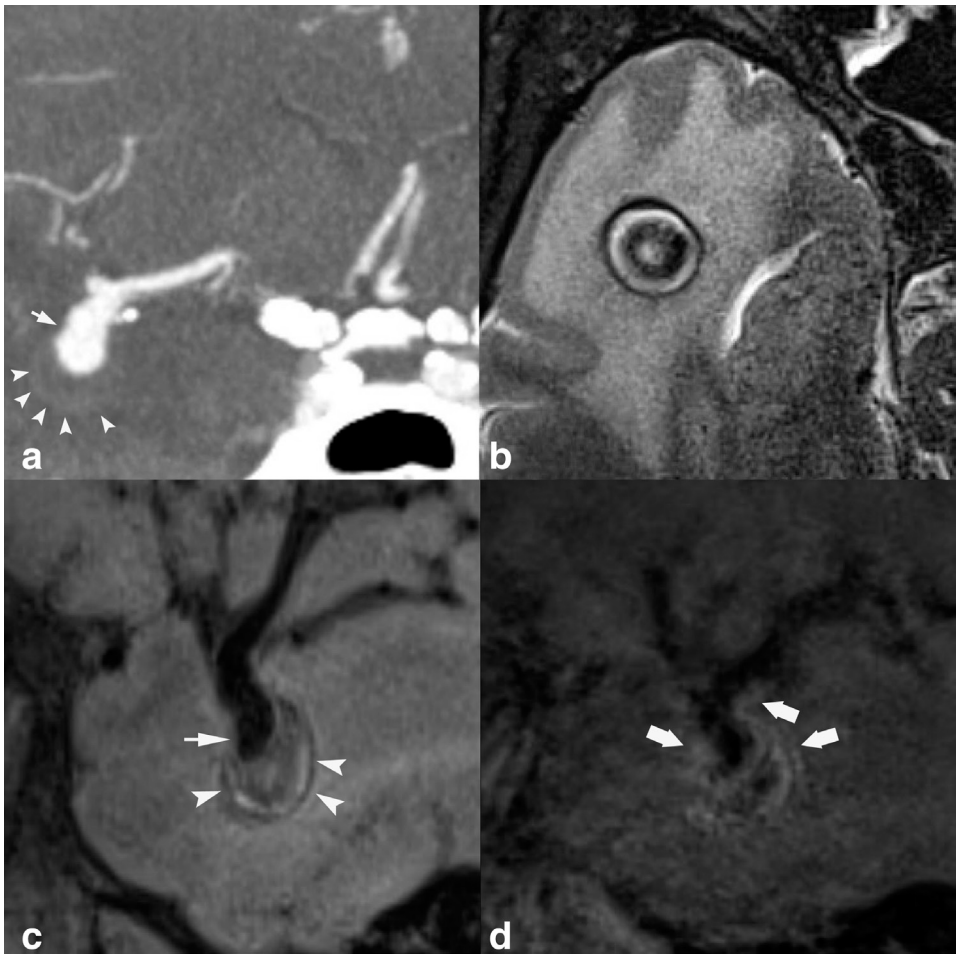

conventional imaging techniques[62] for associations with subsequent vasospasm would be helpful to refine imaging algorithms in the setting of aneurysmal subarachnoid hemorrhage, as vessel wall enhancement could serve as a marker for subsequent vasospasm development and guide preventive treatment if further validated.

HR-VWI can help aneurysm thrombus workup.[63–65] A partially thrombosed aneurysm has a multi-lamellated "onion skin" appearance, with layers of variable signal intensity thrombus on T_1 and T_2-weighted HR-VWI, with areas of T1 hyper- and iso-intensity, and mixed T2 hypo- and hyper-intensity (Figure 6). AWE can also be seen on HR-VWI in partially or completely thrombosed aneurysms. Since the thrombosed portion may enlarge regardless of the lumen size, it is of added value to be able to visualize the lumen, thrombus and aneurysm wall independently, which can be achieved by the use of HR-VWI.[66]

There are a number of potential pitfalls that exist with HR-VWI. Slow or turbulent flow can lead to loss of blood signal suppression, which is exacerbated on post-contrast T_1-weighted sequences due to shortening of the inversion time, and can lead to the false appearance of AWE.[9,31,33] Slow flow can be normally found at the periphery of normal arteries by virtue of the parabolic velocity curve. Turbulent flow can be seen in a number of pathological processes, including in the setting of arterial stenoses, within aneurysm sacs or an arteriovenous malformation nidus. With lower resolution imaging, venous structures in close proximity to an aneurysm may be misconstrued as aneurysm wall enhancement, as veins will frequently show artifactual wall and luminal enhancement secondary to slow venous flow and loss of blood suppression. Moreover, some sites of AWE can be challenging to assess especially those in close proximity to the dura or within the cavernous sinus due to venous enhancement that can obscure wall assessment.[67] AWE should be assessed in multiple planes considering that tangential planes have been shown to overestimate enhancement.[68]

Figure 7. 48-year-old with unruptured 4 mm anterior communicating aneurysm. Computational fluid dynamic Time averaged wall shear stress map shows a prominent region of reduced wall shear stress involving one of the aneurysm lobes (arrow).

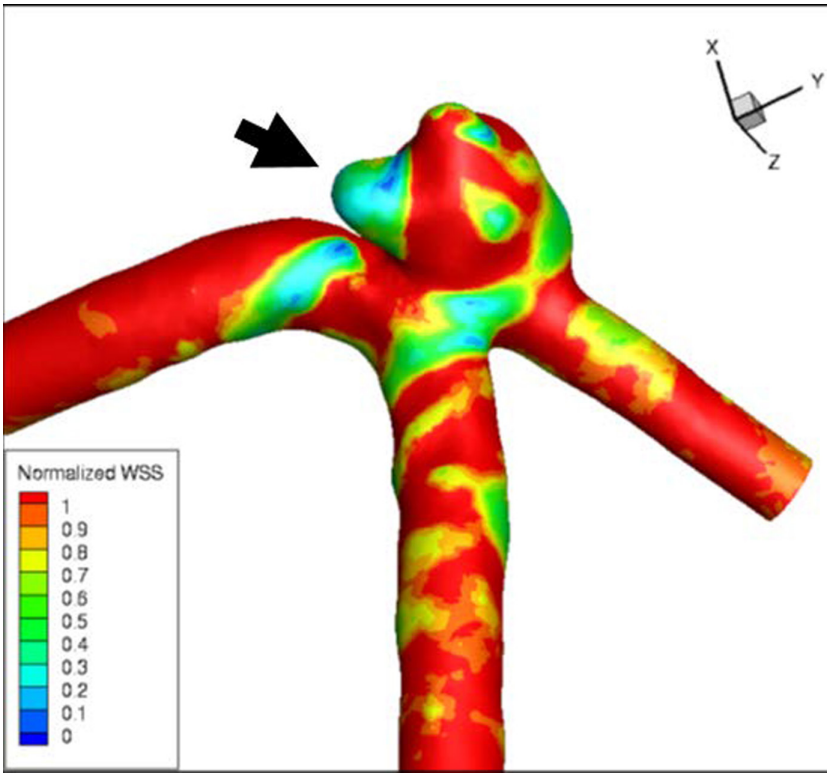

Hemodynamic imaging: Computational fluid dynamic simulations and 4D-Flow MRI

Hemodynamic flow associated with cerebral aneurysms has been shown to be a major cause for aneurysm formation, growth, and rupture.[69,70] Advanced techniques that can be used to evaluate hemodynamic parameters of cerebral aneurysms include 4D-CTA and 4D-flow MRI, while post-processing techniques such as computational fluid dynamics (CFD), can use 3D luminal data (CTA, MRA, DSA) combined with normative or actual flow data to generate simulations to calculate hemodynamic parameters.[71] While many hemodynamic parameters have been investigated for CFD, the main parameters include Wall Shear Stress, Oscillatory Shear Index, Pressure Difference, and Pressure Loss Coefficient.[71]

Wall Shear Stress (WSS) is a frictional force on the arterial wall produced by blood flow in a direction toward a local tangent plane and is impacted by blood viscosity.[71] This leads to formation of a boundary layer adjacent to arterial wall, a layer of fluid where flow velocity is zero, with a gradient of velocities to the center of the lumen, where there is maximum velocity. Controversial results of both high and low WSS (Figure 7)[70,72] have shown correlation with aneurysm rupture. Meng et al[73] indicated that the variability of the association of aneurysm rupture and WSS characteristics resulted from differences in aneurysm phenotypes and pathophysiological mechanisms of rupture. High WSS may be related to mural cell–mediated destructive remodeling, which can cause aneurysm rupture from mural cell damage.[74] High WSS has also shown an association with aneurysm initiation and growth from these pathophysiological changes.[74,75] On the other hand, low WSS is associated with regions of aneurysm dome wall thinning, with low WSS being an independent correlate with wall thinning on ROC analysis.[76] WSS more commonly, however, may vary during the development and progression of an aneurysm as well, with high WSS contributing to aneurysm formation, and as the aneurysm grows, changes in local environment result in low WSS within the aneurysm sac, leading to an endothelial inflammatory response, extracellular matrix degradation and continued aneurysm progression.[75]

Oscillatory Shear Index (OSI)[71] measures the directional changes of WSS during the cardiac cycle. OSI becomes larger with greater angle changes of WSS direction and is often used to describe the disturbance of a flow field. Previous studies reported that a higher OSI was observed in ruptured than in unruptured aneurysms, or high OSI corresponded to the rupture point.[56]

Pressure difference (Pd) was calculated by subtracting the average pressure (Pave) from the maximum pressure (Pmax) and normalized by dividing this by the dynamic pressure at the aneurysm inlet side. Suzuki et al[77] evaluated 23 saccular MCA bifurcation aneurysms, and suggested high Pd combined with low WSS at the Pmax area is a useful hemodynamic parameter for differentiating rupture status. Another study found that the maximum Pd corresponded to aneurysm wall thinning in 82.0%, which further indicates its relationship with aneurysm rupture risk.[78]

Figure 8. A patient presenting with headache. On CTA MIP reconstructed image in oblique plane (A), and axial CTA source image (B) there is an unruptured anterior communicating artery aneurysm (arrows) that has focal lobulation along its left side (arrowheads). 4D-CTA frames (C) show a focal protuberance at the dome of the aneurysm (arrowheads), that disappears on subsequent frames (thick arrow), indicating irregular pulsation. The maximum perpendicular height of the focal temporary protuberance was 1.1 mm.

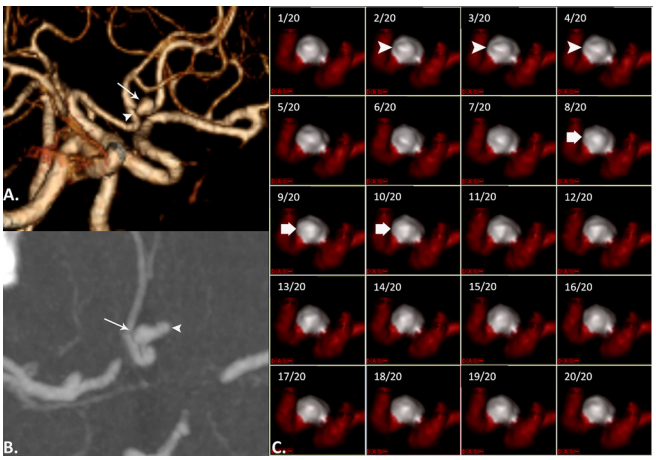

The pressure loss coefficient (PLc) calculates pressure loss associated with course of blood flow. Pathways with resistance to flow, such as tortuous arterial course or aneurysm flow can contribute to increased PLc.[71] PLc has been shown to be reduced in ruptured aneurysms compared to UIAs.[79] It is hypothesized that high PLc contributes to aneurysm remodeling and growth, leading to hemodynamic stabilization, however, the morphological changes contribute to aneurysm instability.[79]

There are several limitations of CFD.[71] First, most large CFD studies only use morphological aneurysm data and otherwise rely on normative patient information. Patient physiological information such as blood pressure, flow velocity, blood viscosity, and heart rate are usually fixed as a uniform condition. The simulations assume the arterial wall to be rigid, and blood is considered as a Newtonian fluid with specific values of density and viscosity. These assumptions and use of normative data can lead to inaccurate simulation output, as these variables differ from patient to patient, and anatomic abnormalities, including aneurysm irregularity, can result in non-Newtonian flow. These shortcomings have limited the application of CFD as a clinical decision-making tool in assessing flow and its impact on vascular pathology.[75]

Individual 2D phase-contrast MRI imaging slices have been traditionally used to evaluate blood flow, however, these acquisitions can be time-consuming, especially when considering complex, multidirectional intracranial vasculature. 2D phase-contrast can also be of limited value due to the small number of arteries that can be sampled in a single imaging session. Recently, however, 4D-flow MRI or time-resolved 3D phase-contrast velocity mapping has been introduced, which is 3D spatial encoding combined with three-directional velocity-encoded Phase contrast MRI to evaluate more detailed flow information.[80,81] 4D-flow allows for accurate hemodynamic information based on true flow velocity data, producing accurate measures of WSS, pressure differences and other hemodynamic parameters. 4D-flow has shown good reproducibility and inter- and intrareader reliability.[82,83] Compared to CFD simulations, 4D-flow closely approximates intraaneurysmal flow patterns in different aneurysm morphologies.[84–86] Limitations of 4D-flow include longer image acquisition times and lower spatial and temporal resolution. Another challenge of hemodynamic assessments, including CFD and 4D-flow is the lack of consensus on which metrics to rely on for evaluation of aneurysm stability/instability, which is a result of the large volume of hemodynamic data and parameters generated. Technological advancements to improve spatiotemporal resolution and overcome some of the 4D-flow limitations include k-t parallel imaging acceleration, compressed sensing, and simultaneous encoding of two Venc measures.[80,83] With continued advancements and prospective validation, 4D-flow has the potential to provide imaging markers for aneurysm stability that can contribute to clinical decision-making.

Four-Dimensional CTA

4D-CTA can evaluate aneurysm wall motion, and thus identify focal, irregular, disconjugate pulsation (Figure 8), which is significantly associated with shape change on follow-up CTA,[87] wall thinning during intraoperative evaluation,[88] higher rupture risk[89] and aneurysm rupture.[90] Zhang et al[89] reviewed 117 aneurysms, 48 of which showed irregular wall motion, defined as ≥1 mm temporary focal wall protuberance lasting for at least three consecutive frames. Aneurysms with irregular wall motion had more than a 6-fold higher 1 year and 5 year rupture risk (2.4 and 1.56%, respectively) compared to aneurysms without irregular wall motion (0.4 and 0.23%, respectively) ($p < .001$). In a separate study, the same group looked at 328 aneurysms (37 ruptured, 60 symptomatic, and 231 asymptomatic), and found that irregular aneurysm wall motion was an independent association with aneurysm symptomatic/ruptured status (OR 5.03; 95% CI 2.83–8.92). For UIAs, irregular wall motion was independently associated with aneurysm symptoms (OR 6.31; 95% CI 3.02–13.2). Hayakawa et al[87] studied 62 UIAs who underwent baseline 4D-CTA with follow-up conventional CTA performed after more than 120 days, and found those with irregular aneurysm wall pulsation were significantly more likely to have morphological aneurysm changes on follow-up CTA than without aneurysm wall pulsation ($p = .04$).

Incorporation into clinical practice

Table 1 compares conventional and advanced aneurysm imaging techniques. At our institution, we have employed HR-VWI into clinical practice. We also perform HR-VWI in small or suspicious aneurysms, to inform potential aneurysm instability that would not otherwise be evaluable. Aneurysms characteristics on HR-VWI, in combination with additional clinical information, may push towards more aggressive treatment or follow-up. Conversely, aneurysms without enhancement, may be followed less frequently. HR-VWI is routinely performed after aneurysm treatment, to potentially predict risk of vasospasm development and guide prophylactic calcium-channel blocker therapy.

Table 1. Benefits of advanced and conventional aneurysm imaging modalities

	HR-VWI	4D-flow MRI	CFD Simulations	4D-CTA	Conventional CTA	Conventional MRA
Pathophysiological data on wall inflammation	+++	-	-	-	-	-
Dynamic wall motion information	-	-	-	+++	_	-
Morphologic information (size, anatomy, irregular shape, dimensions)	++	+	++	+++	+++	++
Hemodynamic flow information	+	+++	+++	-	-	-
Aneurysm origin	++	+	++	++	+++	++
Anatomic relationships	++	+	++	+++	+++	++
Thrombus detection	+++	-	-	++	++	++

4D-CTA has been used, although not with consistency, and 4D-flow and CFD simulations are currently not used clinically.

CONCLUSION

Evaluation of intracranial aneurysms by advanced imaging modalities is emerging as a useful method to guide treatment approaches. HR-VWI, 4D-flow, 4D-CTA, and CFD simulations can be used in combination with patient factors and aneurysmal factors to determine the rupture risk of an aneurysm. In the future, limitations to each technique must be overcome to improve their applicability, and prospective studies are needed to assess their diagnostic value.

REFERENCES

1. Vlak MH, Algra A, Brandenburg R, Rinkel GJ. Prevalence of unruptured intracranial aneurysms, with emphasis on sex, age, comorbidity, country, and time period: a systematic review and meta-analysis. *Lancet Neurol* 2011; **10**: 626–36. https://doi.org/10.1016/S1474-4422(11)70109-0
2. Karamanakos PN, von Und Zu Fraunberg M, Bendel S, Huttunen T, Kurki M, Hernesniemi J, et al. Risk factors for three phases of 12-month mortality in 1657 patients from a defined population after acute aneurysmal subarachnoid hemorrhage. *World Neurosurg* 2012; **78**: 631–39. https://doi.org/10.1016/j.wneu.2011.08.033
3. Etminan N, Rinkel GJ. Unruptured intracranial aneurysms: development, rupture and preventive management. *Nat Rev Neurol* 2016; **12**: 699–713. https://doi.org/10.1038/nrneurol.2016.150
4. Greving JP, Wermer MJH, Brown RD, Morita A, Juvela S, Yonekura M, et al. Development of the phases score for prediction of risk of rupture of intracranial aneurysms: a pooled analysis of six prospective cohort studies. *Lancet Neurol* 2014; **13**: 59–66. https://doi.org/10.1016/S1474-4422(13)70263-1
5. Bijlenga P, Gondar R, Schilling S, Morel S, Hirsch S, Cuony J, et al. Phases score for the management of intracranial aneurysm: a cross-sectional population-based retrospective study. *Stroke* 2017; **48**: 2105–12. https://doi.org/10.1161/STROKEAHA.117.017391
6. Wang Y, Cheng M, Liu S, Xie G, Liu L, Wu X, et al. Shape related features of intracranial aneurysm are associated with rupture status in a large Chinese cohort. *J Neurointerv Surg* 2022; **14**: 252–56. https://doi.org/10.1136/neurintsurg-2021-017452
7. Zhao L, Zhang L, Zhang X, Li Z, Tian L, Wang Y-X. An analysis of 1256 cases of sporadic ruptured cerebral aneurysm in a single chinese institution. *PLoS One* 2014; **9**(1): e85668. https://doi.org/10.1371/journal.pone.0085668
8. Bijlenga P, Gondar R, Schilling S, Morel S, Hirsch S, Cuony J, et al. Phases score for the management of intracranial aneurysm: a cross-sectional population-based retrospective study. *Stroke* 2017; **48**: 2105–12. https://doi.org/10.1161/STROKEAHA.117.017391
9. Santarosa C, Cord B, Koo A, Bhogal P, Malhotra A, Payabvash S, et al. Vessel wall magnetic resonance imaging in intracranial aneurysms: principles and emerging clinical applications. *Interv Neuroradiol* 2020; **26**: 135–46. https://doi.org/10.1177/1591019919891297
10. Lehman VT, Brinjikji W, Kallmes DF, Huston J Rd, Lanzino G, Rabinstein AA, et al. Clinical interpretation of high-resolution vessel wall MRI of intracranial arterial diseases. *Br J Radiol* 2016; **89**: 20160496: 1067: . https://doi.org/10.1259/bjr.20160496
11. Villablanca JP, Duckwiler GR, Jahan R, Tateshima S, Martin NA, Frazee J, et al. Natural history of asymptomatic unruptured cerebral aneurysms evaluated at CT angiography: growth and rupture incidence and correlation with epidemiologic risk factors. *Radiology* 2013; **269**: 258–65. https://doi.org/10.1148/radiol.13121188
12. Rinkel GJE. Intracranial aneurysm screening: indications and advice for practice. *Lancet Neurol* 2005; **4**: 122–28. https://doi.org/10.1016/S1474-4422(05)00993-2
13. White PM, Wardlaw JM, Easton V. Can noninvasive imaging accurately depict intracranial aneurysms? A systematic review. *Radiology* 2000; **217**: 361–70. https://doi.org/10.1148/radiology.217.2.r00nv06361

14. White PM, Teasdale EM, Wardlaw JM, Easton V. Intracranial aneurysms: CT angiography and MR angiography for detection prospective blinded comparison in a large patient cohort. *Radiology* 2001; **219**: 739–49. https://doi.org/10.1148/radiology.219.3.r01ma16739
15. Philipp LR, McCracken DJ, McCracken CE, Halani SH, Lovasik BP, Salehani AA, et al. Comparison between cta and digital subtraction angiography in the diagnosis of ruptured aneurysms. *Neurosurgery* 2017; **80**: 769–77. https://doi.org/10.1093/neuros/nyw113
16. McDonald JS, McDonald RJ, Williamson EE, Kallmes DF. Is intravenous administration of iodixanol associated with increased risk of acute kidney injury, dialysis, or mortality? A propensity score-adjusted study. *Radiology* 2017; **285**: 414–24. https://doi.org/10.1148/radiol.2017161573
17. Su T-H, Hsieh C-H, Chan Y-L, Wong Y-C, Kuo C-F, Li C-H, et al. Intravenous CT contrast media and acute kidney injury: a multicenter emergency department-based study. *Radiology* 2021; **301**: 571–81. https://doi.org/10.1148/radiol.2021204446
18. Ajiboye N, Chalouhi N, Starke RM, Zanaty M, Bell R. Unruptured cerebral aneurysms: evaluation and management. *ScientificWorldJournal* 2015; **2015**: 954954. https://doi.org/10.1155/2015/954954
19. Mandell DM, Mossa-Basha M, Qiao Y, Hess CP, Hui F, Matouk C, et al. Intracranial vessel wall MRI: principles and expert consensus recommendations of the American Society of Neuroradiology. *AJNR Am J Neuroradiol* 2017; **38**: 218–29. https://doi.org/10.3174/ajnr.A4893
20. Mossa-Basha M, Watase H, Sun J, Shibata DK, Hippe DS, Balu N, et al. Inter-rater and scan–rescan reproducibility of the detection of intracranial atherosclerosis on contrast-enhanced 3D vessel wall MRI. *BJR* 2019; **92**: 20180973. https://doi.org/10.1259/bjr.20180973
21. Sarikaya B, Colip C, Hwang WD, Hippe DS, Zhu C, Sun J, et al. Comparison of time-of-flight Mr angiography and intracranial vessel wall MRI for luminal measurements relative to CT angiography. *Br J Radiol* 2021; **94**: 20200743: 1118: . https://doi.org/10.1259/bjr.20200743
22. Brinjikji W, Mossa-Basha M, Huston J, Rabinstein AA, Lanzino G, Lehman VT. Intracranial vessel wall imaging for evaluation of steno-occlusive diseases and intracranial aneurysms. *J Neuroradiol* 2017; **44**: 123–34. https://doi.org/10.1016/j.neurad.2016.10.003
23. de Havenon A, Yuan C, Tirschwell D, Hatsukami T, Anzai Y, Becker K, et al. Nonstenotic culprit plaque: the utility of high-resolution vessel wall MRI of intracranial vessels after ischemic stroke. *Case Rep Radiol* 2015; **2015**: 356582. https://doi.org/10.1155/2015/356582
24. Tian X, Tian B, Shi Z, Wu X, Peng W, Zhang X, et al. Assessment of intracranial atherosclerotic plaques using 3D black-blood MRI: comparison with 3D time-of-flight MRA and DSA. *J Magn Reson Imaging* 2021; **53**: 469–78. https://doi.org/10.1002/jmri.27341
25. Mossa-Basha M, de Havenon A, Becker KJ, Hallam DK, Levitt MR, Cohen WA, et al. Added value of vessel wall magnetic resonance imaging in the differentiation of moyamoya vasculopathies in a non-Asian cohort. *Stroke* 2016; **47**: 1782–88. https://doi.org/10.1161/STROKEAHA.116.013320
26. Mossa-Basha M, Hwang WD, De Havenon A, Hippe D, Balu N, Becker KJ, et al. Multicontrast high-resolution vessel wall magnetic resonance imaging and its value in differentiating intracranial vasculopathic processes. *Stroke* 2015; **46**: 1567–73. https://doi.org/10.1161/STROKEAHA.115.009037
27. Mossa-Basha M, Shibata DK, Hallam DK, de Havenon A, Hippe DS, Becker KJ, et al. Added value of vessel wall magnetic resonance imaging for differentiation of nonocclusive intracranial vasculopathies. *Stroke* 2017; **48**: 3026–33. https://doi.org/10.1161/STROKEAHA.117.018227
28. Mossa-Basha M, Zhu C, Yuan C, Saba L, Saloner DA, Edjlali M, et al. Survey of the American Society of Neuroradiology membership on the use and value of intracranial vessel wall MRI. *AJNR Am J Neuroradiol* 2022; **43**: 951–57. https://doi.org/10.3174/ajnr.A7541
29. Zhu C, Wang X, Eisenmenger L, Tian B, Liu Q, Degnan AJ, et al. Surveillance of unruptured intracranial saccular aneurysms using noncontrast 3D-black-blood MRI: comparison of 3D-TOF and contrast-enhanced MRA with 3D-DSA. *AJNR Am J Neuroradiol* 2019; **40**: 960–66. https://doi.org/10.3174/ajnr.A6080
30. Balu N, Zhou Z, Hippe DS, Hatsukami T, Mossa-Basha M, Yuan C. Accelerated multi-contrast high isotropic resolution 3D intracranial vessel wall MRI using a tailored k-space undersampling and partially parallel reconstruction strategy. *MAGMA* 2019; **32**: 343–57. https://doi.org/10.1007/s10334-018-0730-8
31. Kalsoum E, Chabernaud Negrier A, Tuilier T, Benaïssa A, Blanc R, Gallas S, et al. Blood flow mimicking aneurysmal wall enhancement: a diagnostic pitfall of vessel wall MRI using the postcontrast 3D turbo spin-echo MR imaging sequence. *AJNR Am J Neuroradiol* 2018; **39**: 1065–67. https://doi.org/10.3174/ajnr.A5616
32. Qiao Y, Steinman DA, Qin Q, Etesami M, Schär M, Astor BC, et al. Intracranial arterial wall imaging using three-dimensional high isotropic resolution black blood MRI at 3.0 Tesla. *J Magn Reson Imaging* 2011; **34**: 22–30. https://doi.org/10.1002/jmri.22592
33. Sannananja B, Zhu C, Colip CG, Somasundaram A, Ibrahim M, Khrisat T, et al. Image-quality assessment of 3D intracranial vessel wall MRI using DANTE or DANTE-CAIPI for blood suppression and imaging acceleration. *AJNR Am J Neuroradiol* 2022; **43**: 837–43. https://doi.org/10.3174/ajnr.A7531
34. Lehman VT, Brinjikji W, Mossa-Basha M, Lanzino G, Rabinstein AA, Kallmes DF, et al. Conventional and high-resolution vessel wall MRI of intracranial aneurysms: current concepts and new horizons. *J Neurosurg* 2018; **128**: 969–81. https://doi.org/10.3171/2016.12.JNS162262
35. Feng J, Liu X, Zhang Z, Wu Y, Li Z, Zhang Q, et al. Comparison of 7 T and 3 T vessel wall MRI for the evaluation of intracranial aneurysm wall. *Eur Radiol* 2022; **32**: 2384–92. https://doi.org/10.1007/s00330-021-08331-9
36. Liu X, Feng J, Li Z, Zhang Z, Zhang Q, Jiang Y, et al. Quantitative analysis of unruptured intracranial aneurysm wall thickness and enhancement using 7T high resolution, black blood magnetic resonance imaging. *J Neurointerv Surg* 2022; **14**: 723–28. https://doi.org/10.1136/neurintsurg-2021-017688
37. Liu X, Zhang Z, Zhu C, Feng J, Liu P, Kong Q, et al. Wall enhancement of intracranial saccular and fusiform aneurysms may differ in intensity and extension: a pilot study using 7-T high-resolution black-blood MRI. *Eur Radiol* 2020; **30**: 301–7. https://doi.org/10.1007/s00330-019-06275-9
38. Sherif C, Kleinpeter G, Loyoddin M, Mach G, Plasenzotti R, Haider T, et al. Aneurysm wall thickness measurements of experimental aneurysms: in vivo high-field MR imaging versus direct microscopy. *Acta Neurochir Suppl* 2015; **120**: 17–20. https://doi.org/10.1007/978-3-319-04981-6_3
39. Hartman JB, Watase H, Sun J, Hippe DS, Kim L, Levitt M, et al. Intracranial aneurysms at higher clinical risk for rupture demonstrate increased wall enhancement and thinning on multicontrast 3D vessel wall MRI. *Br J Radiol* 2019; **92**: 20180950: 1096: . https://doi.org/10.1259/bjr.20180950

40. Edjlali M, Guédon A, Ben Hassen W, Boulouis G, Benzakoun J, Rodriguez-Régent C, et al. Circumferential thick enhancement at vessel wall MRI has high specificity for intracranial aneurysm instability. *Radiology* 2018; **289**: 181–87. https://doi.org/10.1148/radiol.2018172879
41. Fu Q, Wang Y, Zhang Y, Zhang Y, Guo X, Xu H, et al. Qualitative and quantitative wall enhancement on magnetic resonance imaging is associated with symptoms of unruptured intracranial aneurysms. *Stroke* 2021; **52**: 213–22. https://doi.org/10.1161/STROKEAHA.120.029685
42. Hasan D, Chalouhi N, Jabbour P, Dumont AS, Kung DK, Magnotta VA, et al. Early change in ferumoxytol-enhanced magnetic resonance imaging signal suggests unstable human cerebral aneurysm: a pilot study. *Stroke* 2012; **43**: 3258–65. https://doi.org/10.1161/STROKEAHA.112.673400
43. Kang H, Tian D-C, Yang X, Zhang Y, Li W, Sui B, et al. A randomized controlled trial of statins to reduce inflammation in unruptured cerebral aneurysms. *JACC Cardiovasc Imaging* 2022; **15**: 1668–70. https://doi.org/10.1016/j.jcmg.2022.04.006
44. Liu P, Qi H, Liu A, Lv X, Jiang Y, Zhao X, et al. Relationship between aneurysm wall enhancement and conventional risk factors in patients with unruptured intracranial aneurysms: a black-blood MRI study. *Interv Neuroradiol* 2016; **22**: 501–5. https://doi.org/10.1177/1591019916653252
45. Matouk CC, Mandell DM, Günel M, Bulsara KR, Malhotra A, Hebert R, et al. Vessel wall magnetic resonance imaging identifies the site of rupture in patients with multiple intracranial aneurysms: proof of principle. *Neurosurgery* 2013; **72**: 492–96. https://doi.org/10.1227/NEU.0b013e31827d1012
46. Zhu C, Mossa-Basha M. Wall enhancement as an emerging marker of intracranial aneurysm stability: roadmap toward a potential target for clinical trials. *Eur J Neurol* 2021; **28**: 3550–51. https://doi.org/10.1111/ene.15094
47. Shimonaga K, Matsushige T, Ishii D, Sakamoto S, Hosogai M, Kawasumi T, et al. Clinicopathological insights from vessel wall imaging of unruptured intracranial aneurysms. *Stroke* 2018; **49**: 2516–19. https://doi.org/10.1161/STROKEAHA.118.021819
48. Zhong W, Su W, Li T, Tan X, Chen C, Wang Q, et al. Aneurysm wall enhancement in unruptured intracranial aneurysms: a histopathological evaluation. *J Am Heart Assoc* 2021; **10**(2): e018633. https://doi.org/10.1161/JAHA.120.018633
49. Samaniego EA, Roa JA, Hasan D. Vessel wall imaging in intracranial aneurysms. *J Neurointerv Surg* 2019; **11**: 1105–12. https://doi.org/10.1136/neurintsurg-2019-014938
50. Matsushige T, Shimonaga K, Mizoue T, Hosogai M, Hashimoto Y, Kaneko M, et al. Focal aneurysm wall enhancement on magnetic resonance imaging indicates intraluminal thrombus and the rupture point. *World Neurosurg* 2019; **127**: e578. https://doi.org/10.1016/j.wneu.2019.03.209
51. Quan K, Song J, Yang Z, Wang D, An Q, Huang L, et al. Validation of wall enhancement as a new imaging biomarker of unruptured cerebral aneurysm. *Stroke* 2019; **50**: 1570–73. https://doi.org/10.1161/STROKEAHA.118.024195
52. Edjlali M, Gentric J-C, Régent-Rodriguez C, Trystram D, Hassen WB, Lion S, et al. Does aneurysmal wall enhancement on vessel wall MRI help to distinguish stable from unstable intracranial aneurysms? *Stroke* 2014; **45**: 3704–6. https://doi.org/10.1161/STROKEAHA.114.006626
53. Texakalidis P, Hilditch CA, Lehman V, Lanzino G, Pereira VM, Brinjikji W. Vessel wall imaging of intracranial aneurysms: systematic review and meta-analysis. *World Neurosurg* 2018; **117**: 453–58. https://doi.org/10.1016/j.wneu.2018.06.008
54. Ishibashi T, Murayama Y, Urashima M, Saguchi T, Ebara M, Arakawa H, et al. Unruptured intracranial aneurysms: incidence of rupture and risk factors. *Stroke* 2009; **40**: 313–16. https://doi.org/10.1161/STROKEAHA.108.521674
55. Nasr DM, Flemming KD, Lanzino G, Cloft HJ, Kallmes DF, Murad MH, et al. Natural history of vertebrobasilar dolichoectatic and fusiform aneurysms: a systematic review and meta-analysis. *Cerebrovasc Dis* 2018; **45**: 68–77. https://doi.org/10.1159/000486866
56. Juvela S. Risk factors for multiple intracranial aneurysms. *Stroke* 2000; **31**: 392–97. https://doi.org/10.1161/01.str.31.2.392
57. Nagahata S, Nagahata M, Obara M, Kondo R, Minagawa N, Sato S, et al. Wall enhancement of the intracranial aneurysms revealed by magnetic resonance vessel wall imaging using three-dimensional turbo spin-echo sequence with motion-sensitized driven-equilibrium: a sign of ruptured aneurysm? *Clin Neuroradiol* 2016; **26**: 277–83. https://doi.org/10.1007/s00062-014-0353-z
58. Krings T, Lasjaunias PL, Geibprasert S, Pereira V, Hans FJ. The aneurysmal wall. the key to a subclassification of intracranial arterial aneurysm vasculopathies? *Interv Neuroradiol* 2008; **14 Suppl 1**: 39–47. https://doi.org/10.1177/15910199080140S107
59. Yoshikawa K, Moroi J, Kokubun K, Furuya N, Yoshida Y, Kinoshita T, et al. Role of magnetic resonance vessel wall imaging in detecting and managing ruptured aneurysms among multiple intracranial aneurysms. *Surg Neurol Int* 2021; **12**: 460. https://doi.org/10.25259/SNI_618_2021
60. Mossa-Basha M, Huynh TJ, Hippe DS, Fata P, Morton RP, Levitt MR. Vessel wall MRI characteristics of endovascularly treated aneurysms: association with angiographic vasospasm. *J Neurosurg* 2018; **131**: 859–67. https://doi.org/10.3171/2018.4.JNS172829
61. Hsu CC-T, Suthiphosuwan S, Huynh T, Murphy A, Li Y, Bharatha A. High-Resolution MRI vessel wall imaging in acute aneurysmal subarachnoid hemorrhage: spatiotemporal pattern and clinicoradiologic implications. *Clin Neuroradiol* 2020; **30**: 801–10. https://doi.org/10.1007/s00062-019-00843-8
62. Colip CG, Wo S, Hippe DS, Watase H, Urdaneta-Moncada AR, Zhu C, et al. Computed tomography angiography findings predictive of post-intervention vasospasm in patients with aneurysmal subarachnoid hemorrhage. *Br J Radiol* 2021; **94**: 20200893: 1121: . https://doi.org/10.1259/bjr.20200893
63. Matsubara S, Hadeishi H, Suzuki A, Yasui N, Nishimura H. Incidence and risk factors for the growth of unruptured cerebral aneurysms: observation using serial computerized tomography angiography. *J Neurosurg* 2004; **101**: 908–14. https://doi.org/10.3171/jns.2004.101.6.0908
64. Sato T, Matsushige T, Chen B, Gembruch O, Dammann P, Jabbarli R, et al. Wall contrast enhancement of thrombosed intracranial aneurysms at 7T MRI. *AJNR Am J Neuroradiol* 2019; **40**: 1106–11. https://doi.org/10.3174/ajnr.A6084
65. van Gijn J, Rinkel GJ. Subarachnoid haemorrhage: diagnosis, causes and management. *Brain* 2001; **124**: 249–78. https://doi.org/10.1093/brain/124.2.249
66. Martin AJ, Hetts SW, Dillon WP, Higashida RT, Halbach V, Dowd CF, et al. Mr imaging of partially thrombosed cerebral aneurysms: characteristics and evolution. *AJNR Am J Neuroradiol* 2011; **32**: 346–51. https://doi.org/10.3174/ajnr.A2298
67. Portanova A, Hakakian N, Mikulis DJ, Virmani R, Abdalla WMA, Wasserman BA. Intracranial vasa vasorum: insights and implications for imaging. *Radiology* 2013; **267**: 667–79. https://doi.org/10.1148/radiol.13112310
68. Alexander MD, Yuan C, Rutman A, Tirschwell DL, Palagallo G, Gandhi D, et al. High-Resolution intracranial vessel wall imaging: imaging beyond the lumen. *J Neurol Neurosurg Psychiatry* 2016; **87**: 589–97. https://doi.org/10.1136/jnnp-2015-312020

69. Cebral J, Ollikainen E, Chung BJ, Mut F, Sippola V, Jahromi BR, et al. Flow conditions in the intracranial aneurysm lumen are associated with inflammation and degenerative changes of the aneurysm wall. *AJNR Am J Neuroradiol* 2017; **38**: 119–26. https://doi.org/10.3174/ajnr.A4951
70. Soldozy S, Norat P, Elsarrag M, Chatrath A, Costello JS, Sokolowski JD, et al. The biophysical role of hemodynamics in the pathogenesis of cerebral aneurysm formation and rupture. *Neurosurg Focus* 2019; **47**: E11. https://doi.org/10.3171/2019.4.FOCUS19232
71. Murayama Y, Fujimura S, Suzuki T, Takao H. Computational fluid dynamics as a risk assessment tool for aneurysm rupture. *Neurosurg Focus* 2019; **47**: E122019.4.FOCUS19189. https://doi.org/10.3171/2019.4.FOCUS19189
72. Sforza DM, Putman CM, Cebral JR. Hemodynamics of cerebral aneurysms. *Annu Rev Fluid Mech* 2009; **41**: 91–107. https://doi.org/10.1146/annurev.fluid.40.111406.102126
73. Meng H, Tutino VM, Xiang J, Siddiqui A. High WSS or low WSS? complex interactions of hemodynamics with intracranial aneurysm initiation, growth, and rupture: toward a unifying hypothesis. *AJNR Am J Neuroradiol* 2014; **35**: 1254–62. https://doi.org/10.3174/ajnr.A3558
74. Zimny M, Kawlewska E, Hebda A, Wolański W, Ładziński P, Kaspera W. Wall shear stress gradient is independently associated with middle cerebral artery aneurysm development: a case-control CFD patient-specific study based on 77 patients. *BMC Neurol* 2021; **21**(1): 281. https://doi.org/10.1186/s12883-021-02251-3
75. Szajer J, Ho-Shon K. A comparison of 4D flow MRI-derived wall shear stress with computational fluid dynamics methods for intracranial aneurysms and carotid bifurcations - A review. *Magn Reson Imaging* 2018; **48**: 62–69. https://doi.org/10.1016/j.mri.2017.12.005
76. Kadasi LM, Dent WC, Malek AM. Colocalization of thin-walled dome regions with low hemodynamic wall shear stress in unruptured cerebral aneurysms. *J Neurosurg* 2013; **119**: 172–79. https://doi.org/10.3171/2013.2.JNS12968
77. Suzuki T, Stapleton CJ, Koch MJ, Tanaka K, Fujimura S, Suzuki T, et al. Decreased wall shear stress at high-pressure areas predicts the rupture point in ruptured intracranial aneurysms. *J Neurosurg* 2019; **132**: 2018.12.JNS182897: 1116–22: . https://doi.org/10.3171/2018.12.JNS182897
78. Suzuki T, Takao H, Suzuki T, Kambayashi Y, Watanabe M, Sakamoto H, et al. Determining the presence of thin-walled regions at high-pressure areas in unruptured cerebral aneurysms by using computational fluid dynamics. *Neurosurgery* 2016; **79**: 589–95. https://doi.org/10.1227/NEU.0000000000001232
79. Takao H, Murayama Y, Otsuka S, Qian Y, Mohamed A, Masuda S, et al. Hemodynamic differences between unruptured and ruptured intracranial aneurysms during observation. *Stroke* 2012; **43**: 1436–39. https://doi.org/10.1161/STROKEAHA.111.640995
80. Markl M, Frydrychowicz A, Kozerke S, Hope M, Wieben O. 4D flow MRI. *J Magn Reson Imaging* 2012; **36**: 1015–36. https://doi.org/10.1002/jmri.23632
81. Youn SW, Lee J. From 2D to 4D phase-contrast MRI in the neurovascular system: will it be a quantum jump or a fancy decoration? *J Magn Reson Imaging* 2022; **55**: 347–72. https://doi.org/10.1002/jmri.27430
82. Markl M, Wallis W, Harloff A. Reproducibility of flow and wall shear stress analysis using flow-sensitive four-dimensional MRI. *J Magn Reson Imaging* 2011; **33**: 988–94. https://doi.org/10.1002/jmri.22519
83. Wentland AL, Grist TM, Wieben O. Repeatability and internal consistency of abdominal 2D and 4D phase contrast mr flow measurements. *Acad Radiol* 2013; **20**: 699–704. https://doi.org/10.1016/j.acra.2012.12.019
84. Castle-Kirszbaum M, Maingard J, Lim RP, Barras CD, Kok HK, Chandra RV, et al. Four-Dimensional magnetic resonance imaging assessment of intracranial aneurysms: a state-of-the-art review. *Neurosurgery* 2020; **87**: 453–65. https://doi.org/10.1093/neuros/nyaa021
85. Maupu C, Lebas H, Boulaftali Y. Imaging modalities for intracranial aneurysm: more than meets the eye. *Front Cardiovasc Med* 2022; **9**: 793072. https://doi.org/10.3389/fcvm.2022.793072
86. Misaki K, Futami K, Uno T, Nambu I, Yoshikawa A, Kamide T, et al. Inflow hemodynamics of intracranial aneurysms: a comparison of computational fluid dynamics and 4D flow magnetic resonance imaging. *J Stroke Cerebrovasc Dis* 2021; **30**: S1052-3057(21)00088-4: 105685: . https://doi.org/10.1016/j.jstrokecerebrovasdis.2021.105685
87. Hayakawa M, Tanaka T, Sadato A, Adachi K, Ito K, Hattori N, et al. Detection of pulsation in unruptured cerebral aneurysms by ECG-gated 3D-CT angiography (4D-CTA) with 320-row area detector CT (ADCT) and follow-up evaluation results: assessment based on heart rate at the time of scanning. *Clin Neuroradiol* 2014; **24**: 145–50. https://doi.org/10.1007/s00062-013-0236-8
88. Ferrari F, Cirillo L, Calbucci F, Bartiromo F, Ambrosetto P, Fioravanti A, et al. Wall motion at 4D-CT angiography and surgical correlation in unruptured intracranial aneurysms: a pilot study. *J Neurosurg Sci* 2019; **63**: 501–8. https://doi.org/10.23736/S0390-5616.16.03640-7
89. Zhang J, Li X, Zhao B, Zhang J, Sun B, Wang L, et al. Irregular pulsation of intracranial unruptured aneurysm detected by four-dimensional CT angiography is associated with increased estimated rupture risk and conventional risk factors. *J Neurointerv Surg* 2021; **13**: 854–59. https://doi.org/10.1136/neurintsurg-2020-016811
90. Zhang J, Li X, Zhao B, Zhang J, Sun B, Wang L, et al. Irregular pulsation of aneurysmal wall is associated with symptomatic and ruptured intracranial aneurysms. *J Neurointerv Surg* 2022: neurintsurg-2021-018381. https://doi.org/10.1136/neurintsurg-2021-018381